Biomedical Signal Processing and Control 85 (2023) 104936

Contents lists available at ScienceDirect

Biomedical Signal Processing and Control

journal homepage: www.elsevier.com/locate/bspc

Decoding transient sEMG data for intent motion recognition in transhumeral amputees

Andrea Tigrini [a,*], Ali H. Al-Timemy [b], Federica Verdini [a], Sandro Fioretti [a], Micaela Morettini [a], Laura Burattini [a], Alessandro Mengarelli [a]

[a] Department of Information Engineering, Università Politecnica delle Marche, Ancona, Italy
[b] Biomedical Engineering Department, Al-Khwarizmi College of Engineering, University of Baghdad, Baghdad, Iraq

ARTICLE INFO

Keywords:
Myoelectric control
Transient sEMG
Pattern recognition
Shoulder joint
Transhumeral amputees

ABSTRACT

The use of surface electromyographic (sEMG) signals, alongside pattern recognition (PR) systems, is fundamental in the design and control of assistive technologies. Transient sEMG signal epochs at the early beginning of the movement provide important information for upper-limb intent of motion recognition. However, only few studies investigated the role of transient sEMG for myoelectric control architectures. Therefore, in this work, focus was given to transient sEMG signals of intact-limb (IL) subjects and transhumeral amputees (AMP), who performed a series of shoulder movements. The role of the window length for feature extraction was investigated by sub-windowing the transient epochs at 200, 150, 100, and 50 ms window length (WL). Gaussian kernel discriminant analysis (SRKDA) and support vector machine (SVM) were used for recognizing seven classes of motion at different hold-out percentage of training/testing data, i.e. 70%–30%, 60%–40% and 50%–50%. In all the latter conditions, the median classification accuracy and F1 score were greater than 80% for both IL and AMP groups when using SRKDA. Wilcoxon rank sum test was employed to verify possible differences between WL conditions. Although the latter did not show significant differences, 100 ms WL showed the best classification performances for both groups (classification accuracy greater than 90%, near that of a usable PR system). Results demonstrated that a reliable motion intent recognition of shoulder joint in transhumeral amputee patients can be obtained employing transient sEMG epochs. This can be used in a better design of myoelectric control architectures of assistive technologies, involving the upper-limb for clinical use.

1. Introduction

Although the recognition of hand gestures is one of the most investigated topic in the development of myoelectric interfaces s [1–4] through surface electromyographic (sEMG) signals, it should be highlighted that other joint motions start to be deeply investigated for myoelectric control, such as the shoulder [5–8]. Under such framework of applications, the decoding of shoulder degrees of freedom is paramount [9–11], and robust pattern recognition architectures (PRA), able to provide good recognition performances on limited EMG windows, are becoming central in the development of control policies for assistive technologies involving shoulder joint [6,9,12]. Indeed, the delivery of an assistive action by the device can occur only if the motion intent is properly decoded [13,14]. For this reason the majority of the studies focused on the classification of static sEMG epochs [9,13,14], hence admitting a certain amount of delay between the effective decoding of the neuromuscular control command and the actuation of task delivered by the machine. On the other hand, relative few studies took into account the role of transient sEMG epochs which can be observed at the early beginning of the movement [6,11,12,15]. The importance of dealing with transient EMG epochs is twofold. Firstly, they demonstrated to be relevant for the prediction of the human intent of motion [8,11,16]. Secondly, transient EMG windows guarantee a reduced delays in the control loop, hence improving the control of assistive technologies [6,12,16].

However, even if transient sEMG signal epochs showed important information for the improvement of PRA-based myoelectric control architectures [15], only recently it has been observed an increased interest in the field [11,16–18]. Transient sEMG provided good capability in predicting the force developed by the forearm [17], but also for generalizing and improving the algorithms for hand prosthesis control [16,18]. In [11], sEMG transient epochs classification were considered for the shoulder movements of healthy young population,

* Corresponding author.
E-mail address: a.tigrini@staff.univpm.it (A. Tigrini).

https://doi.org/10.1016/j.bspc.2023.104936
Received 31 October 2022; Received in revised form 18 March 2023; Accepted 5 April 2023
Available online 13 April 2023

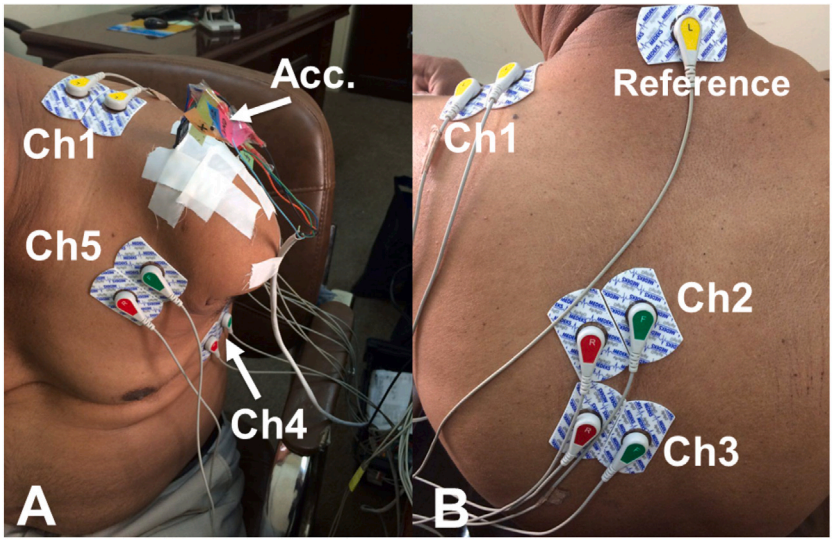

Fig. 1. The electrodes position on an amputee subject. Panel A and B show respectively the frontal and back view of the electrodes location. Channel 1 (Ch1) acquired the myoelectric activity of the upper fibers of the trapezius, whereas Ch3 the lower ones. Ch2 was placed on the Rhomboid major. Ch4 and Ch5 were placed respectively on the Serratus Anterior and on the Pectoralis minor. All the muscle activity was differentially recorded with respect to the reference electrode. The accelerometer was placed on the shoulder (panel A) to measure the acceleration of the joint, permitting a precise segmentation of the data.

in order to understand the role of time and frequency domain features for the classification of the aforementioned signal epochs. Although good classification performances were obtained, the investigation of only healthy population limits the development of myoelectric-based assistive technologies.

A further element of interest regards the role of the window length (WL) for feature extraction and classification of sEMG transient epochs [19]. This was partially investigated in the myoelectric control literature, and deserves to be developed in order to improve PRA for real time purposes. In fact, although the role of WL has been investigated for hand gesture recognition using sparse or dense set-up [20,21], only marginal contributions were given to the proper selection of WL when one deals with transient sEMG epochs. It is important to emphasize that the myoelectric PRA here investigated dealt with transient sEMG data, which are of crucial importance in decoding human motion intent [6,12,19], but also in the estimation of muscle force development in the upper limb [17], or in the generalization of PRA for prosthetic control [15,18].

Hence, the aim of this study is twofold. At first, the early decoding the principal shoulder movements in healthy and amputee subjects by using transient sEMG data was investigated. Secondly, the role of WL for feature extraction was analyzed for transient sEMG signals.

2. Materials and methods

2.1. Experimental protocol

The dataset collected in [22] was used in this study. Ten subjects, i.e. four transhumeral amputees (AMP) and six intact-limb (IL) subjects were recruited for the experiment. The subjects gave their consent for the experiment which was conducted under the declaration of Helsinki and its later amendments [22].

Each subject was instrumented with 5 sEMG differential channels (Fig. 1) to record the myoelectric activity of the upper and lower fibers of the Trapezious (UTR and LTR), the Rhomboid major (RM), the Serratus anterior (SA) and the Pectoralis minor (PM), following the instructions proposed in [23]. Moreover, a 3-axis accelerometer was placed on the shoulder, providing the three acceleration components of the joint in the local reference frame [10,22]. Both accelerometer and sEMG signals were acquired synchronously at a rate of 1000 Hz, with NI USB-6009 (National Instruments, USA).

Table 1
Table reports the labels of the shoulder movements performed during the trials by both the AMP and IL populations.

Shoulder movement	Label
Elevation	EL
Depression	DE
Protraction	PT
Retraction	RT
Upward rotation	UR
Downward rotation	DR

For each acquisition trial, AMP and IL subjects performed 6 shoulder movements as reported in Table 1. Subjects were asked to maintain the final joint configuration for 5 s during each movement [22]. The first four movements were performed sequentially, whereas a resting phase of 5 s was required before the execution of the fifth and sixth movements. The adoption of the aforementioned procedure was guided by the need of limiting both the recording time and the rise of fatigue, avoiding also possible stress effects that can be given by fully sequential movements or prolonged acquisitions. Eventually, a total of 8 trials data relative to the 6 shoulder movements described in Table 1 were available for each subject belonging to the AMP and IL cohorts.

2.2. Signal pre-processing and segmentation

The sEMG signals were filtered through a fourth-order, zero-phase, band-pass filter in the range of 30–450 Hz [6,11], whereas the three-component accelerometer data were band-pass filtered between 2 and 20 Hz. Then, such components were used to compute the time course of the acceleration magnitude through the following equation:

$$A(t) = \sqrt{A_x(t)^2 + A_y(t)^2 + A_y(t)^2} \quad (1)$$

where A is the magnitude of the acceleration at a given time t, whereas A_x, A_y, and A_z are respectively the three acceleration components at the time t, each properly referred to the relative accelerometer axis. The obtained $A(t)$ signal showed clear step-transitions when the shoulder movements started and ended for both AMP and IL groups as reported in Fig. 2. For the identification of each shoulder movement onset, we applied a single-threshold detector, computing the average value (TH) and the standard deviation (SD) of $A(t)$ on a 2 s window before

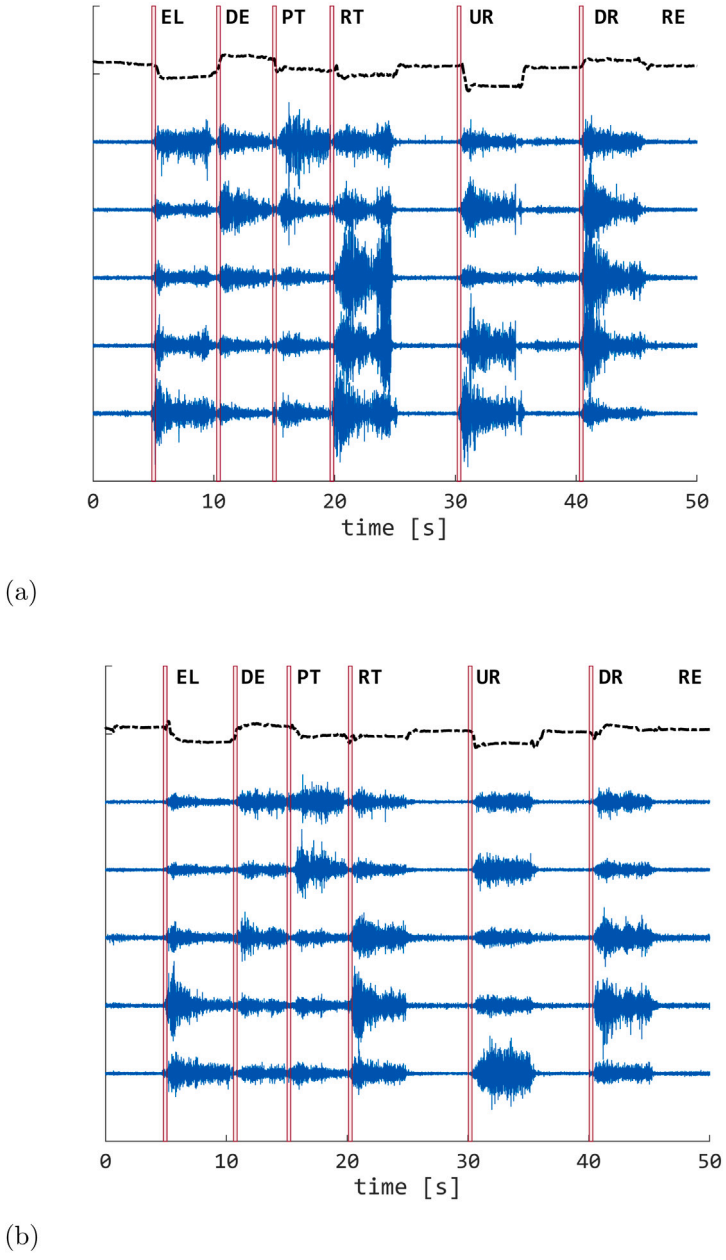

Fig. 2. Example of the five sEMG signals (blue line) recorded for a given trial of one IL and one AMP subject (respectively panel 2(a) and 2(b)). The dashed black lines show the acceleration magnitude used to identify the six movements onset. Red areas highlight the 300 ms transient windows representing the MID windows used for feature extraction.

any movement onset. Then, we identified the time instant where $A(t)$ magnitude rise above or below a value equal to $TH \pm 3 \cdot SD$. If $A(t)$ remained above or below the latter value for at least 0.05 s, the time instant identified at the beginning of the procedure was retained as the actual movement onset. The goodness of the entire process was finally checked by visual inspection, resulting suitable for motion intent detection (MID) windows definition [11,19]. This procedure allowed to avoid the use of cumbersome optometric or force measurement systems previously used to identify movements onset [11,13]. Thus accordingly with the literature [11,12], MID windows of 300 ms were centered at each movement onset to segment the sEMG signal epochs (see Fig. 2).

For each subject, a total of 8 (trials) × 6 (movements) × 5 (channels) of sEMG signal epochs of 300 ms were extracted as the MID windows, and they underwent to feature extraction. Moreover, also the class "rest" was defined in order to properly train the myoelectric PRA [9,10]. Thus, an additive MID window was considered by segmenting the last 300 ms of sEMG activity of each trial. As shown in Fig. 2, no motion was present in the final part of the recordings. This guaranteed the definition of a well balanced dataset, where the amount of sEMG data to extract the features representing the rest class (RE) was the same employed for the actual shoulder motion classes (see Table 1).

2.3. Pattern recognition experiments

Features in the time domain that guaranteed the implementation of reliable PRA models were aggregated to compute the feature set [21,24,25]. In particular, the mean absolute value (MAV), zero crossing (ZC), slope sign change (SSC), waveform length (WL), variance (VAR), Willison amplitude (WAMP), and the four coefficients of a fourth-order auto-regressive process were selected as data descriptors. Hereafter, the aggregation of the aforementioned features is indicated as TDAR feature set [21]. Furthermore, as indicated in Section 1, in order to investigate the role of WL for transient sEMG epochs, in this study four different sub-windowing for feature extraction were investigated.

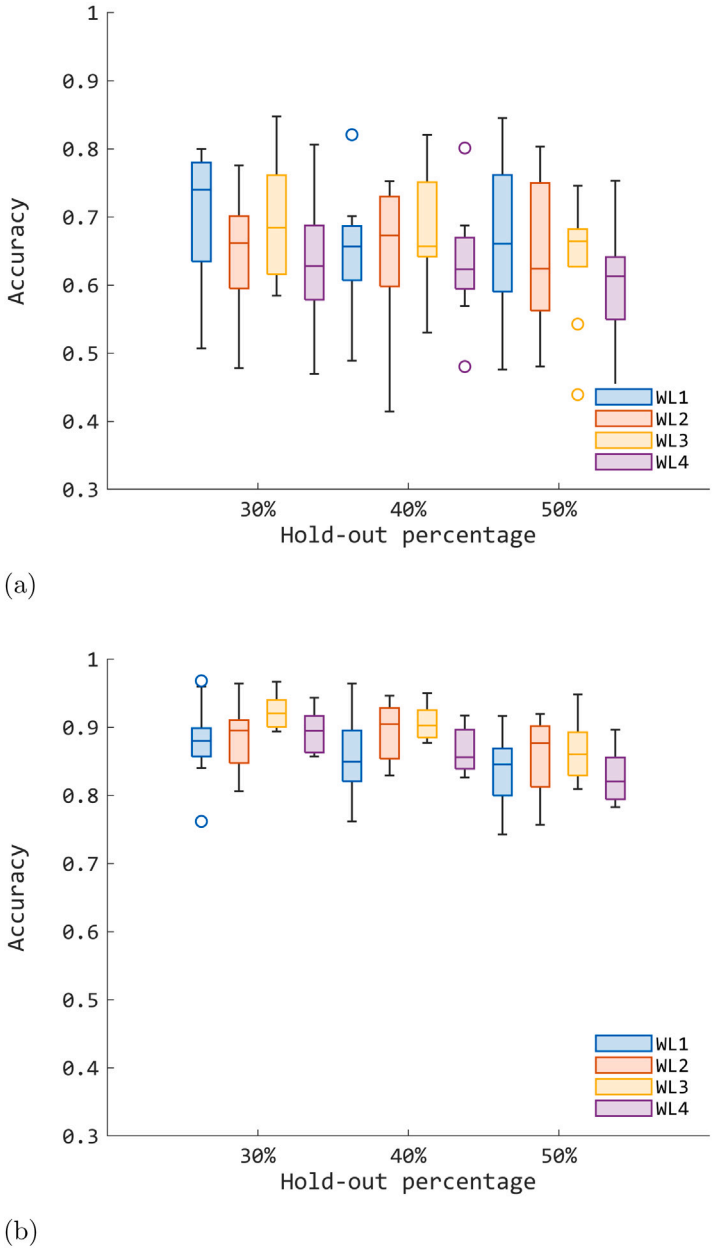

Fig. 3. WSA of SVM and SRKDA for the entire population are shown in panel 3(a) and 3(b), respectively. Box-plots of the two metrics obtained in the three different testing conditions, i.e. 30%, 40% and 50% held out data, where reported with respect to the four WL employed.

Hence, sliding windows of 200 (WL1), 150 (WL2), 100 (WL3), and 50 (WL4) ms, with an overlap of 75%, were employed to extract the TDAR feature set.

For each subject in the IL and AMP groups, all the labeled signal epochs were employed to extract the TDAR at the three different WL, which were used to generate within-subject PRA models. In the literature, no indications regarding the use of a specific classifier was found to boost the accuracy when one deals with transient sEMG data [11,16]. However, multi-class support vector machine (SVM) with linear kernel was efficiently employed in two studies related to hand gesture and wrist movement classification for prosthetic control with transient sEMG data [16,26]. Hence, such PRA was selected as a first viable model for decoding the motion intent of the shoulder joint. In addition to linear SVM model, a kernel discriminant analysis (KDA) was also selected since it showed reliable performances as both classifier and dimensionality reduction method [27,28]. A brief recall of the KDA is reported in the following. Let consider a dataset made by m samples $\boldsymbol{x}_1, \boldsymbol{x}_2, \ldots, \boldsymbol{x}_m \in \mathbb{R}^n$ belonging to c classes. Considering the classification problem in a feature space $\mathcal{F}$ induced by an opportune nonlinear map $\phi(\cdot) : \mathbb{R}^n \mapsto \mathcal{F}$ such that an inner product $\langle ; \rangle$ on this space can be defined. In particular, the map can be selected to make $\mathcal{F}$ a reproducing kernel Hilbert space for which $\langle \phi(\boldsymbol{x}_i); \phi(\boldsymbol{x}_j) \rangle = \mathcal{K}(\boldsymbol{x}_i, \boldsymbol{x}_j)$, where $\mathcal{K}(;)$ is a positive semi-definite kernel function. As shown in [29], the KDA training can be formally considered as an optimization problem of the form:

$$\arg\max_{\boldsymbol{\alpha}} \quad \frac{\boldsymbol{\alpha}^T K W K \boldsymbol{\alpha}}{\boldsymbol{\alpha}^T K K \boldsymbol{\alpha}} \tag{2}$$

where K is the kernel matrix while W is a weighting matrix defined as follow:

$$\begin{cases} \frac{1}{m_k}; \text{ if } \boldsymbol{x}_i \text{ and } \boldsymbol{x}_j \text{ both belong to the } k\text{th class} \\ 0; \text{ otherwise} \end{cases} \tag{3}$$

with m_k equals to the number of points present in the kth class [29]. It is possible to see that the optimal vector $\boldsymbol{\alpha}$ can be obtained by solving

the following eigen-problem:

$$KWK\alpha = KK\alpha \tag{4}$$

However, as highlighted in [29,30], rather than solve the eigen-problem shown in (4) through an eigen decomposition of the matrix K [31], which may require a high computational burden, a spectral regression formulation (SRKDA) was employed to obtain a solution of the aforementioned eigen-problem. All the details regarding the implementation of SRKDA can be found in [29,30], here it is important to highlight that the spectral regression approach avoids the direct eigen-decomposition of the K matrix by solving a trivial eigen-problem decomposition that involves W and a linear systems that involves K.

To compute the elements of the K matrix, a Gaussian kernel function was employed resulting as follows:

$$K_{ij}(\boldsymbol{x}_i;\boldsymbol{x}_j) = \exp\left(\frac{\|\boldsymbol{x}_i - \boldsymbol{x}_j\|^2}{\sigma}\right) \tag{5}$$

where $\boldsymbol{x}_i$ and $\boldsymbol{x}_j$ represent two given data points in the TDAR feature spaces. The scaling value σ was estimated from the data as the average of the mean values computed from the Euclidean distance matrix, obtained from each couple of feature vectors.

The SVM and SRKDA models were trained using the TDAR feature set computed from WL1 to WL4. Moreover, to test the robustness of the trained PRA, multiple classifiers were trained by randomly splitting the feature sets varying the hold-out percentage of data for testing. Hence, the 70%–30%, 60%–40% and 50%–50% data split conditions for training-testing were investigated respectively. It deserves to be highlighted that the random split implemented in this study keeps the feature sets for training and testing balanced in order to avoid possible biases in the results due to unbalanced classes conditions. Within-subject accuracy (WSA) and F1 Score computed over test sets were employed as metrics to judge the goodness of the PRA models.

2.4. Statistical analysis

A first group of comparisons was performed to assess the quality of each PRA, by taking into account both the hold-out percentage of data and the window length for feature computing. In the first case Wilcoxon rank sum test (WRS) was employed for pairwise comparison of the WSA and F1 scores among each pair of window length conditions by fixing the hold-out percentage of data for testing. These comparisons were set to test whether WL1, WL2, WL3 and WL4 affected or not the performances of both SVM and SRKDA models. Then, WRS was employed to compare WSA and F1 among each pair of hold-out percentage, by fixing the WL condition for both models. This allows to evaluate whether PRA architectures were characterized by over-fitting behavior or they showed good responses even when training was performed with a low amount of data.

In a second group of comparisons, the WRS was used to compare SVM and SRKDA models by fixing the WL and the hold-out percentage. This was done to test which model between the two aforementioned models provided the best classification results in decoding shoulder intent of motion.

3. Results and discussion

Figs. 3 and 4 show respectively the WSA and F1 scores obtained at the different hold-out percentage of testing data for both SVM and SRKDA models. In particular, for SVM models, median accuracy ranges between 0.65 and 0.75 for each hold-out percentage and WL considered, showing also large interquartile ranges (see Fig. 3(a)). The F1 score mirrors the trend showed in the accuracy (see Fig. 4(a)), indicating a high variability of the SVM models in recognizing the shoulder intent of motion. Moreover, the statistical analysis did not show any significant change either with respect to the hold-out percentage or with respect to WL condition. Regarding the SRKDA models, both WSA (Fig. 3(b)) and F1 (Fig. 4(b)) show median values greater than 80% among all the three hold-out conditions and for all the four WLs. The statistical analysis highlighted no significant drop ($p>0.05$) neither when the window length was reduced nor when the testing data were increased (see Section 2.4). Moreover, the F1 score shows comparable behavior with respect to WSA, showing a narrow interquartile range, hence supporting the goodness of the SRKDA models.

Superior performances of SRKDA with respect to SVM was statistically verified for each WL and hold-out percentage for both metrics employed ($p < 0.05$) This further indicates that the SRKDA here designed through transient sEMG epochs showed reliable performances in detecting the intent of shoulder motion for both AMP and IL subjects. This is paramount in the practical context of full upper-limb prosthesis control or in the design of assistive technologies for the upper limb [6,9,12]. On the other hand, the lower performances obtained for the SVM models, if compared also with other studies that dealt with amputee patients [16,26], may be imputed to the use of a sparse and reduced sEMG setup, i.e., 5 probes, that naturally leads to feature space with smaller dimension with respect to other studies [11,16]. Indeed, by construction, SVM performs better with higher dimensional data [32], supporting the line that large feature spaces could be extracted when dealing with reduced set-up and SVM architectures [33,34]. On the other hand, confirmation regarding the goodness of the SRKDA in classifying transient data of both groups can be observed in Fig. 5. Hence, SRKDA was retained as classification model for the following analyses.

Indeed, the performances obtained for the six healthy subjects shared the same range of accuracy with that of the AMP group, showing mean WSA values ranges between 0.85 and 0.90, with slightly superior results obtained for the IL group, aligning with what observed in [26] on transradial amputee patients. Present outcomes agree also with those reported in [8], where the MID problem was faced for patients affected by chronic stroke, showing a median error rate of about 20% for the paretic limb using EMG data only and slightly better results were obtained when other sources of information was used, e.g. load cell recordings. The same level of accuracy (about 80%) was also reported for partially hand amputees [35] but without using transient data and also with a greater number of electrodes, i.e. up to 13. A myoelectric-based human-machine interface was also developed in [13] for patients who suffered from spinal cord injury. Although average accuracy on pathological individuals was comparable with that obtained in this study for transhumeral amputees, it is important to note that, in [13], the WSA showed large variations among patients, falling in some cases under 50%. Conversely, in the present study the WSA presented quite repeatable values for each patients and for each WL (Fig. 5). This aspect is particularly important for a real-usage scenario, since it highlights that also classification architectures trained only with transient data can be reliable for developing myoelectric control interfaces.

Although the statistical analysis did not show differences among the testing or WL conditions, it deserved to be noticed that WL3 guaranteed the best performances in both AMP and IL, whereas lower values were observed in the case of WL4. This is in line with [19], confirming that WL in the range of 200–50 ms can be a good choice for MID problems using sparse sEMG setup. Indeed, to obtain comparable performances in terms of myoelectric control accuracy, with a reduction of the WL, literature suggested the use of high density set-up [21,36]. This however could be a limitation when more classical sparse sEMG probes are the only available option.

A further confirmation regarding the possibility to obtain reliable performances in identifying intent of motion by transient data for transhumeral amputee patients, through sparse probe setup, can be found observing the average confusion matrices for both groups (see Figs. 6 and 7, respectively). The behavior of IL and AMP groups follows a repeatable pattern among the WL conditions, showing fully clean zones outside the first diagonal for WL1 (Figs. 6(b) and 7(b)) and WL2

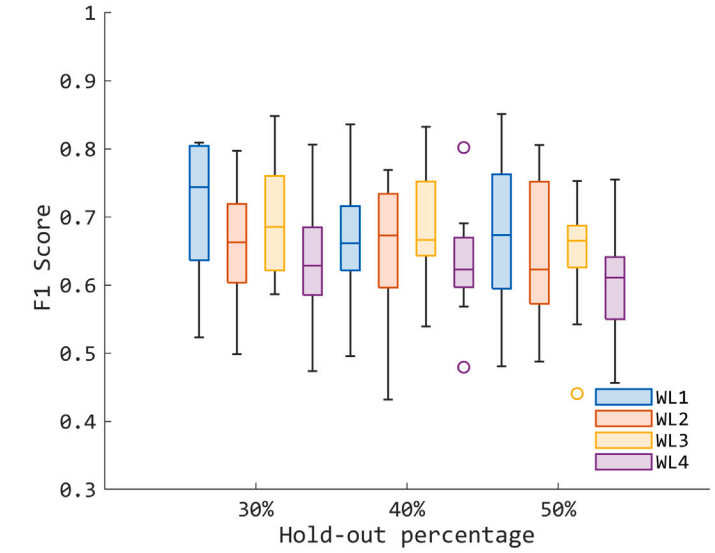

(a)

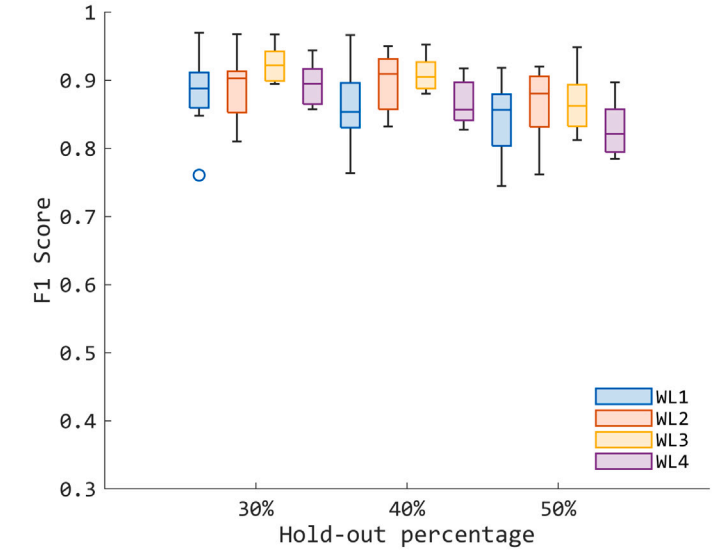

(b)

Fig. 4. F1 score of SVM and SRKDA for the entire population are shown in panel 4(a) and 4(b), respectively. Box-plots of the two metrics obtained in the three different testing conditions, i.e. 30%, 40% and 50% held out data, where reported with respect to the four WL employed.

(Figs. 6(b) and 7(b)). However, for the above mentioned conditions, errors greater than 10% are present, supporting the lower mean accuracy values obtained if compared with respect to WL3 condition (Fig. 5). Indeed, the latter showed the optimal trade off between high principal diagonal classification rate and false rates in the other components of the confusion-charts (Figs. 6(c) and 7(c)) also if compared with WL4, which showed reduced accuracy values in the principal diagonal (Figs. 6(d) and 7(d)). Furthermore, it deserves to be noticed that among the WL conditions, false detection shows no bias due to specific shoulder movements misclassification. Indeed, no clustered false rate zones were identified for AMP and IL groups (see Figs. 6 and 7).

In this study, the effectiveness of pattern classification of transient sEMG epochs was provided for transhumeral amputees, with overall performances not lower with respect to healthy subjects (Fig. 5). This means that also in the case of damaged muscles, transient sEMG epochs can carry information for a proper control of full-limb prosthesis. This can also be confirmed by the example reported in Fig. 8, where an example of testing classifier output signal was reported. Even if a spurious misclassification spike is present, the majority of the transient epoch samples were correctly classified. As highlighted in [3,33], myoelectric PRA performances can be boosted by smoothing classifiers output, either adaptively or under a probabilistic framework [33,37], by applying a post processors to the output of the classifier. Such post processors work in real-time and they are used to clean the decision signal given by PRA from spurious spikes (Fig. 8), eventually making the PRA prototype suitable to be embedded in real-time myoelectric control schemes. Although the implementation of the SRKDA model in a PRA-based controller is beyond the aim of the study, it deserves to be investigated in future works, together with the implementation of majority voting or Bayesian fusion post processing schemes [33,37]. This can allow a boosting of PRA architectures that work with transient data as those presented here and in other studies [11,19,26], in order to improve real-time control performances of assistive technologies.

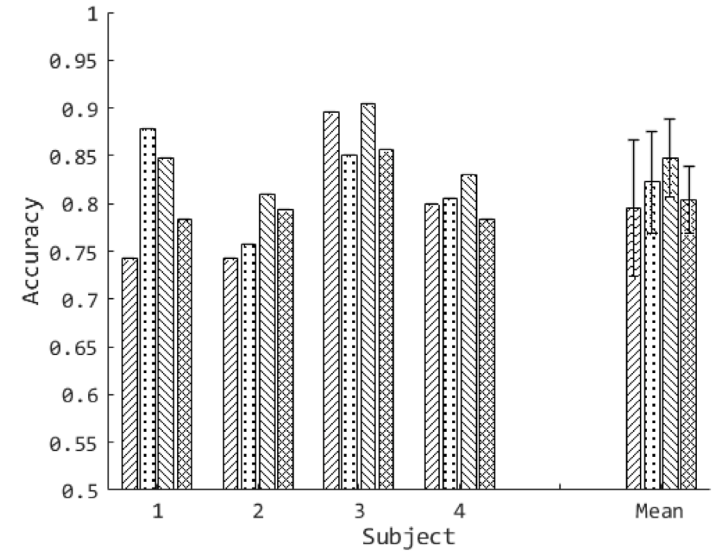

(a)

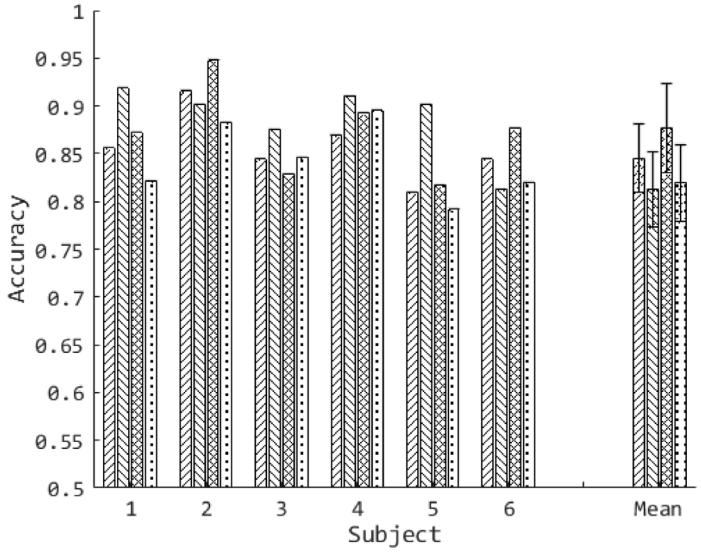

(b)

Fig. 5. WSA obtained in case of 50% hold-out test condition for the AMP (panel 5(a)) and IL (panel 5(b)) groups. Both panels report a final bars group indicating the mean and standard deviation range with respect to the subjects. Right-slanted lines denote WL1, dot hatch indicates WL2, left-slanted lines stand for WL3, and criss-crossing lines denote WL4.

A further point for future studies is suggested by the acquisition protocol since sequence of EL, DE, PT, and RT movements had no rest between the movements, whereas the remaining two (UR and DR) were performed after a resting period (Fig. 2). Despite this acquisition protocol aimed at minimizing the discomfort for the amputee patients, further studies should be devoted to assess whether performing movements sequentially or switching an action after entering a resting state could affect MID classification performances. Eventually, in the conditions of transient sEMG epoch classification, the PRA designed were able to provide good performances using WL for feature extraction up to 50 ms, even with a sparse set-up. This suggests that myoelectric control architectures for motion intent can be fed at a faster rate with respect to about 250 ms, typically employed when dealing with myoelectric pattern recognition.

4. Conclusion

In this study the problem of shoulder motion intent detection was treated employing transient sEMG epochs for IL and AMP groups. The latter showed WSA comparable with the one obtained for IL subjects, highlighting the possibility to develop PRA for MID also in transhumeral amputees. This result is strengthened also by considering that no significant performances drops were observed reducing training data. In addition, also small signal window length resulted suitable for a robust detection of intent of motion in healthy as well as amputee patients. Future studies should involve the investigation of hierarchical PR models, which deal with static and transient sEMG signal epochs. A further point regards the assessment of transient models with static signal epochs and vice versa.

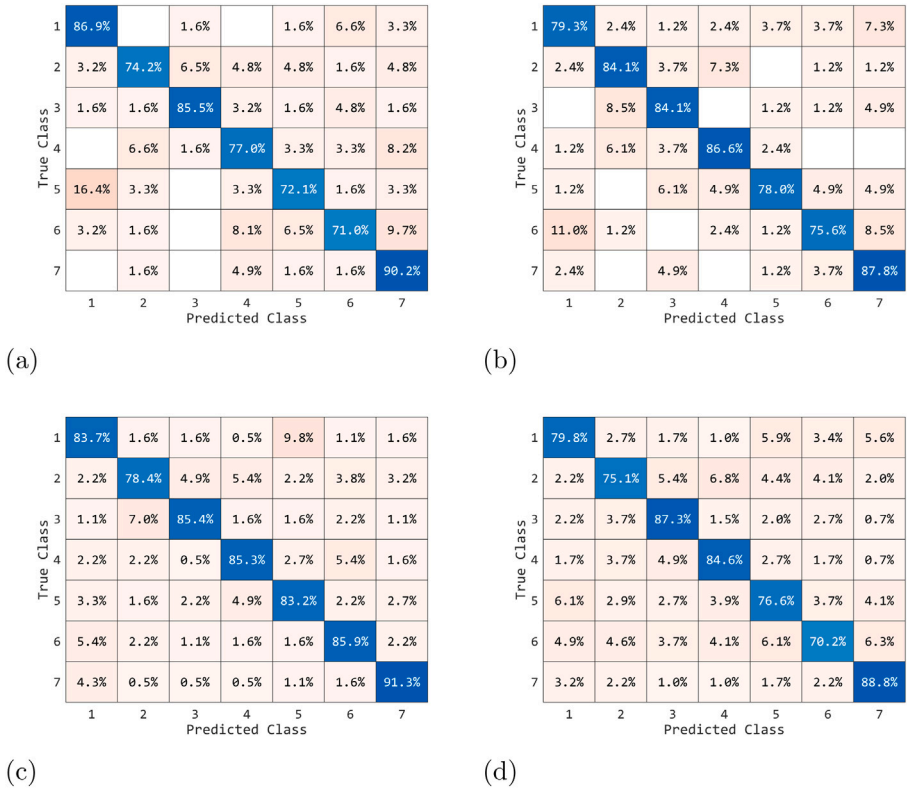

Fig. 6. Average confusion chart obtained in testing of the AMP group for the 50% hold-out condition with SRKDA. Panels 7(a), 7(b), 7(d), and 7(d) refer to WL1, WL2, WL3, and WL4 respectively.

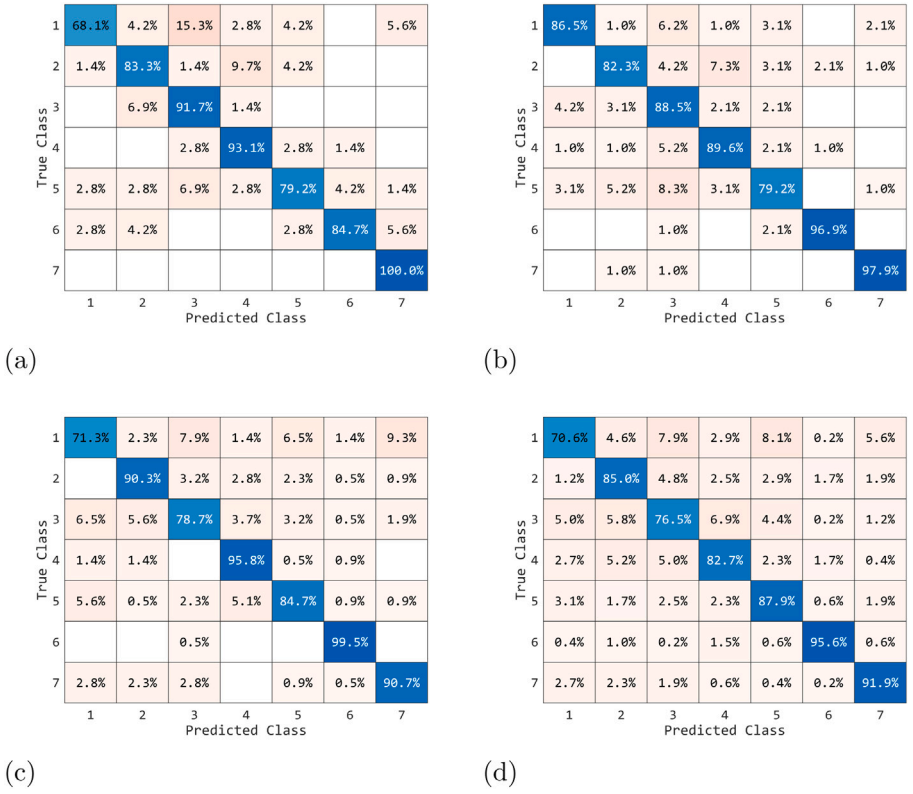

Fig. 7. Average confusion chart obtained in testing of the IL group for the 50% hold-out condition with SRKDA. Panels 7(a), 7(b), 7(d), and 7(d) refer to WL1, WL2, WL3, and WL4 respectively.

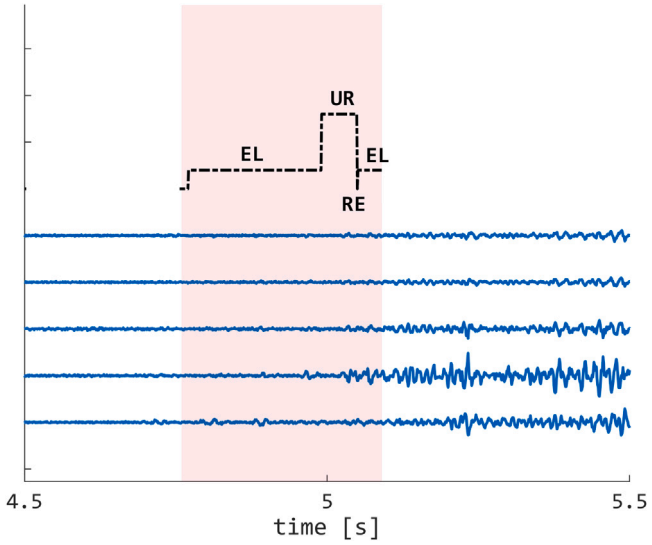

Fig. 8. Testing classification output of an amputee subject performing the first movement (EL). In this case a spurious misclassification between EL and UR and between EL and RE occurred (black dotted line). The majority of the transient epoch samples were correctly identified.

CRediT authorship contribution statement

Andrea Tigrini: Conceptualization, Methodology, Formal analysis, Investigation, Writing – original draft, Writing – review & editing, Visualization. **Ali H. Al-Timemy:** Conceptualization, Methodology, Investigation, Resources, Writing – original draft, Writing – review & editing, Visualization, Supervision. **Federica Verdini:** Conceptualization, Methodology, Formal analysis, Investigation, Writing – original draft, Writing – review & editing, Supervision. **Sandro Fioretti:** Conceptualization, Resources, Writing – review & editing, Visualization. **Micaela Morettini:** Conceptualization, Formal analysis, Writing – review & editing, Visualization. **Laura Burattini:** Conceptualization, Resources, Writing – review & editing, Visualization. **Alessandro Mengarelli:** Conceptualization, Methodology, Investigation, Writing – original draft, Writing – review & editing, Visualization, Supervision.

Declaration of competing interest

The authors declare that they have no known competing financial interests or personal relationships that could have appeared to influence the work reported in this paper.

Data availability

Data will be made available on request.

Acknowledgments

The authors are thankful to Gaith Sharba for providing the dataset used in this study.

References

[1] F. Botros, A. Phinyomark, E. Scheme, EMG-based gesture recognition: Is it time to change focus from the forearm to the wrist? IEEE Trans. Ind. Inform. 18 (1) (2022) 174–184.
[2] A. Mengarelli, A. Tigrini, S. Fioretti, S. Cardarelli, F. Verdini, On the use of fuzzy and permutation entropy in hand gesture characterization from EMG signals: Parameters selection and comparison, Appl. Sci. 10 (20) (2020) 7144.
[3] A.H. Al-Timemy, G. Bugmann, J. Escudero, Adaptive windowing framework for surface electromyogram-based pattern recognition system for transradial amputees, Sensors 18 (8) (2018) 2402.
[4] L. Vargas, H. Huang, Y. Zhu, D. Kamper, X. Hu, Resembled tactile feedback for object recognition using a prosthetic hand, IEEE Robot. Autom. Lett. 7 (4) (2022) 10977–10984.
[5] M. Sierotowicz, D. Brusamento, B. Schirrmeister, M. Connan, J. Bornmann, J. Gonzalez-Vargas, C. Castellini, Unobtrusive, natural support control of an adaptive industrial exoskeleton using force-myography, Front. Robot. AI 223.
[6] E. Trigili, L. Grazi, S. Crea, A. Accogli, J. Carpaneto, S. Micera, N. Vitiello, A. Panarese, Detection of movement onset using EMG signals for upper-limb exoskeletons in reaching tasks, J. Neuroeng. Rehabil. 16 (1) (2019) 1–16.
[7] N. Lotti, M. Xiloyannis, F. Missiroli, C. Bokranz, D. Chiaradia, A. Frisoli, R. Riener, L. Masia, Myoelectric or force control? A comparative study on a soft arm exosuit, IEEE Trans. Robot. (2022).
[8] J.V. Kopke, M.D. Ellis, L.J. Hargrove, Determining user intent of partly dynamic shoulder tasks in individuals with chronic stroke using pattern recognition, IEEE Trans. Neural Syst. Rehabil. Eng. 28 (1) (2020) 350–358.
[9] D. Rivela, A. Scannella, E.E. Pavan, C.A. Frigo, P. Belluco, G. Gini, Analysis and comparison of features and algorithms to classify shoulder movements from sEMG signals, IEEE Sens. J. 18 (9) (2018) 3714–3721.
[10] E. Nsugbe, A.H. Al-Timemy, Shoulder girdle recognition using electrophysiological and low frequency anatomical contraction signals for prosthesis control, CAAI Trans. Intell. Technol. 7 (1) (2022) 81–94.
[11] A. Tigrini, L.A. Pettinari, F. Verdini, S. Fioretti, A. Mengarelli, Shoulder motion intention detection through myoelectric pattern recognition, IEEE Sens. Lett. 5 (8) (2021) 1–4.
[12] B. Cesqui, P. Tropea, S. Micera, H.I. Krebs, EMG-based pattern recognition approach in post stroke robot-aided rehabilitation: A feasibility study, J. Neuroeng. Rehabil. 10 (1) (2013) 1–15.
[13] C.G. McDonald, J.L. Sullivan, T.A. Dennis, M.K. O'Malley, A myoelectric control interface for upper-limb robotic rehabilitation following spinal cord injury, IEEE Trans. Neural Syst. Rehabil. Eng. 28 (4) (2020) 978–987.
[14] A.W. Franzke, M.B. Kristoffersen, V. Jayaram, C.K. van der Sluis, A. Murgia, R.M. Bongers, Exploring the relationship between EMG feature space characteristics and control performance in machine learning myoelectric control, IEEE Trans. Neural Syst. Rehabil. Eng. 29 (2021) 21–30.
[15] T. Lorrain, N. Jiang, D. Farina, Influence of the training set on the accuracy of surface EMG classification in dynamic contractions for the control of multifunction prostheses, J. Neuroeng. Rehabil. 8 (1) (2011) 1–9.
[16] G. Kanitz, C. Cipriani, B.B. Edin, Classification of transient myoelectric signals for the control of multi-grasp hand prostheses, IEEE Trans. Neural Syst. Rehabil. Eng. 26 (9) (2018) 1756–1764.
[17] I.J.R. Martínez, A. Mannini, F. Clemente, C. Cipriani, Online grasp force estimation from the transient EMG, IEEE Trans. Neural Syst. Rehabil. Eng. 28 (10) (2020) 2333–2341.
[18] E. Tyacke, S.P. Reddy, N. Feng, R. Edlabadkar, S. Zhou, J. Patel, Q. Hu, S.F. Atashzar, Hand gesture recognition via transient sEMG using transfer learning of dilated efficient CapsNet: Towards generalization for neurorobotics, IEEE Robot. Autom. Lett. 7 (4) (2022) 9216–9223.
[19] A. Tigrini, M. Scattolini, A. Mengarelli, S. Fioretti, M. Morettini, L. Burattini, F. Verdini, Role of the window length for myoelectric pattern recognition in detecting user intent of motion, in: 2022 IEEE International Symposium on Medical Measurements and Applications, MeMeA, IEEE, 2022, pp. 1–6.
[20] L.H. Smith, L.J. Hargrove, B.A. Lock, T.A. Kuiken, Determining the optimal window length for pattern recognition-based myoelectric control: Balancing the competing effects of classification error and controller delay, IEEE Trans. Neural Syst. Rehabil. Eng. 19 (2) (2011) 186–192.
[21] R.N. Khushaba, K. Nazarpour, Decoding HD-EMG signals for myoelectric control-how small can the analysis window size be? IEEE Robot. Autom. Lett. 6 (4) (2021) 8569–8574.
[22] G.K. Sharba, M.K. Wali, A.H. Al-Timemy, Wavelet-based feature extraction technique for classification of different shoulder girdle motions for high-level upper limb amputees, Int. J. Med. Eng. Inform. 12 (6) (2020) 609–619.
[23] E. Criswell, Cram's Introduction to Surface Electromyography, Jones & Bartlett Publishers, 2010.
[24] H. Huang, H.-B. Xie, J.-Y. Guo, H.-J. Chen, Ant colony optimization-based feature selection method for surface electromyography signals classification, Comput. Biol. Med. 42 (1) (2012) 30–38.
[25] A. Phinyomark, F. Quaine, S. Charbonnier, C. Serviere, F. Tarpin-Bernard, Y. Laurillau, EMG feature evaluation for improving myoelectric pattern recognition robustness, Expert Syst. Appl. 40 (12) (2013) 4832–4840.
[26] D. D'Accolti, K. Dejanovic, L. Cappello, E. Mastinu, M. Ortiz-Catalan, C. Cipriani, Decoding of multiple wrist and hand movements using a transient EMG classifier, IEEE Trans. Neural Syst. Rehabil. Eng. (2022).
[27] S. Mika, G. Ratsch, J. Weston, B. Scholkopf, K.-R. Mullers, Fisher discriminant analysis with kernels, in: Neural Networks for Signal Processing IX: Proceedings of the 1999 IEEE Signal Processing Society Workshop (Cat. No. 98th8468), IEEE, 1999, pp. 41–48.
[28] K. Anam, R.N. Khushaba, A. Al-Jumaily, Two-channel surface electromyography for individual and combined finger movements, in: 2013 35th Annual International Conference of the IEEE Engineering in Medicine and Biology Society, EMBC, IEEE, 2013, pp. 4961–4964.

[29] D. Cai, X. He, J. Han, Efficient kernel discriminant analysis via spectral regression, in: Seventh IEEE International Conference on Data Mining, ICDM 2007, IEEE, 2007, pp. 427–432.
[30] D. Cai, X. He, J. Han, Speed up kernel discriminant analysis, VLDB J. 20 (1) (2011) 21–33.
[31] G. Baudat, F. Anouar, Generalized discriminant analysis using a kernel approach, Neural Comput. 12 (10) (2000) 2385–2404.
[32] C.M. Bishop, N.M. Nasrabadi, Pattern Recognition and Machine Learning, vol. 4, Springer, 2006.
[33] R.N. Khushaba, S. Kodagoda, M. Takruri, G. Dissanayake, Toward improved control of prosthetic fingers using surface electromyogram (EMG) signals, Expert Syst. Appl. 39 (12) (2012) 10731–10738.
[34] V. Ahlawat, R. Thakur, Y. Narayan, Support vector machine based classification improvement for EMG signals using principal component analysis, J. Eng. Appl. Sci. 13 (8) (2018) 6341–6345.
[35] A.A. Adewuyi, L.J. Hargrove, T.A. Kuiken, An analysis of intrinsic and extrinsic hand muscle EMG for improved pattern recognition control, IEEE Trans. Neural Syst. Rehabil. Eng. 24 (4) (2016) 485–494.
[36] A.A. Al Taee, R.N. Khushaba, T. Zia, A. Al-Jumaily, The effectiveness of narrowing the window size for LD & HD EMG channels based on novel deep learning wavelet scattering transform feature extraction approach, in: 2022 44th Annual International Conference of the IEEE Engineering in Medicine & Biology Society, EMBC, 2022, pp. 3698–3701.
[37] K. Englehart, B. Hudgins, A robust, real-time control scheme for multifunction myoelectric control, IEEE Trans. Biomed. Eng. 50 (7) (2003) 848–854.